A route to potent, selective and biased salvinorin chemical space

Sarah J. Hill,[†,1,2] Nathan Dao, [†,1,2] Vuong Q. Dang,[3] Edward L. Stahl,[3] Laura M. Bohn,[3,*] Ryan A. Shenvi[1,2,*]

[1]Department of Chemistry, Scripps Research, La Jolla, California 92037, United States.

[2]Graduate School of Chemical and Biological Sciences, Scripps Research, La Jolla, California 92037, United States.

[3]Department of Molecular Medicine, The Herbert Wertheim UF Scripps Institute for Biomedical Innovation & Technology, Jupiter, Florida 33458, United States

[*]Corresponding authors: rshenvi@scripps.edu, laura.bohn@ufl.edu

[†]These authors contributed equally to this work.

ABSTRACT: The salvinorins serve as templates for next generation analgesics, antipruritics and dissociative hallucinogens via selective and potent agonism of the *kappa*-opioid receptor (KOR). In contrast to most opioids, the salvinorins lack basic amines and bind with high affinity and selectivity via complex polyoxygenated scaffolds that have frustrated deep-seated modification by synthesis. Here we describe a short asymmetric synthesis that relies on a sterically-confined organocatalyst to dissociate acidity from reactivity and effect Robinson annulation of an unactivated nucleophile / unstable electrophile pair. Combined with a cobalt-catalyzed polarized diene-alkyne cycloaddition, the route allows divergent access to a focused library of salvinorins. We appraise the synthesis by its generation of multiple analogs that exceed the potency, selectivity, stability and functional bias of salvinorin A itself.

Evolutionary selection pressures endow small molecule metabolites with properties that are advantageous to drug development,[1] but natural products often frustrate optimization campaigns due to high complexity and low modularity. For example, salvinorin A (Figure 1), a potent and selective KOR agonist (EC_{50} = 0.9 nM, cAMP inhibition; selectivity index >5000 vs. *mu*-opioid receptor, MOR),[2] exhibits a high lipophilic ligand efficiency (LLE = 8; ClogP = 1.6)[3] and rapidly penetrates mammalian brains to cause psychoactive effects at low concentration (*est.* 10 μg total human brain content).[4] Its complexity, however, has not allowed diversification and optimization by total synthesis. Instead, the salvinorins have been subject to extensive semisynthetic optimization campaigns, which limit diversity (see below).[5] These studies have targeted next-generation analgesics and antipruritic agents that rely on the unique physicochemical properties of the salvinorins, which differ markedly from other KOR-selective agonists (Figure 1A), in no small part due to the absence of a basic amine. Since pain relief via agonism of the related MOR leads to dependency and addiction, significant effort has focused on selective targeting of KOR, which has not been associated with addiction and therefore represents a critical research area for pharmaceutical development. More recent recognition that GPCR ligands can mediate 'biased' or 'functionally-selective' signaling has stimulated a search for new KOR-targeting chemotypes with pliable pharmacology that preferentially activate G protein pathways over βarrestin recruitment.[6,7]

Chemical manipulations of isolated SalA have produced analogs with extended blood half-life,[8,9] increased oral bioavailability[10] and expanded receptor pharmacology.[11] Structural diversity and multisite exploration, however, remain limited; only C2 and C16 analogs have met or exceeded the potency SalA.[5] For example, the equipotent C2 thiocyanatoacetate analog, RB64, exhibited G protein-biased signaling over βarrestin via proposed covalent adduction at the site of binding.[12] C16-bromo-salvinorin A, a non-covalent analog, showed functional bias for G protein signaling over βarrestin2 recruitment and promise as an analgesic (bias factor 7.7); translational potential was attenuated, however, by lower efficacy than balanced analogs in pain-related behavioral models, in addition to sedative effects and low metabolic stability associated with the C2 acetate.[13] Metabolic half-life of salvinorins can be enhanced by the C2 *N*-methylacetamide (NMA) modification, which resisted esterase degradation and increased oral bioavailability, but lost 27X KOR/MOR selectivity.[10] A series of ethers at C2 (e.g., MOM) maintained or exceeded SalA potency and selectivity but did not increase oral bioavailability or brain residence time.[9] Whereas SalA shows tolerability in five healthy patient trials, no analog has advanced to disease-modifying clinical trial.[13] De novo synthesis avoids the constraints of the limited reactivity and stability of SalA.

Prior syntheses[14–20] and medicinal chemistry campaigns struggled with the configurational lability of C8, which underwent epimerization (K_{eq} = 2.5) to generate the low potency 8-*epi*-SalA under acidic, basic and thermal conditions.[5] Whereas total syntheses might provide more analogs for property optimization, they have ranged from 16–29 steps (1.3–0.3% yield)[14–22] generated no analogs and retained, by definition, the C8 configurational lability of SalA itself.[22] As a result, two syntheses targeted stabilized SalA scaffolds that would not epimerize. One elegant effort introduced multiple scaffold changes via a stereoselective transannular Michael cascade (see Scheme S8) but resulted in >100X potency loss and no measure of receptor selectivity.[23] Another effort relied on computational modeling[24] to modify the B and C rings and arrive at the analog O6C (**1**, EC_{50} = 3.3 nM),[25] which resisted epimerization and approached the potency of SalA (see Ref 25 and Figure 4 below). Nevertheless, this effort required 13 steps to synthesize racemic material (<1% yield) and was not diversified to analogs. Poor divergency resulted from length and reliance of C-ring closure on an electron-rich arene that was installed 5-steps away from bioactive chemical space, i.e. **1** (see Scheme S11). Greater divergency and brevity was designed via retrosynthetic conjugate addition and Robinson annulation, if the enol of **2** could engage in chemo- and stereoselective reaction with the pendant enal, an acidic vinylogous 1,3-dicarbonyl and unprecedented partner.

Intermediate **2** could derive from 2-acetoxy-Hagemann's ester (**3**) as a scalemic building block. Here we report an asymmetric synthesis of (–)-**1** plus 29 bioactive analogs by diversification of a common scaffold (9 steps, 6.7% overall yield). New structure activity relationships that deliver increased potency, selectivity and C8 stability, in addition to G protein-biased agonism, demonstrate the practicality of the route.

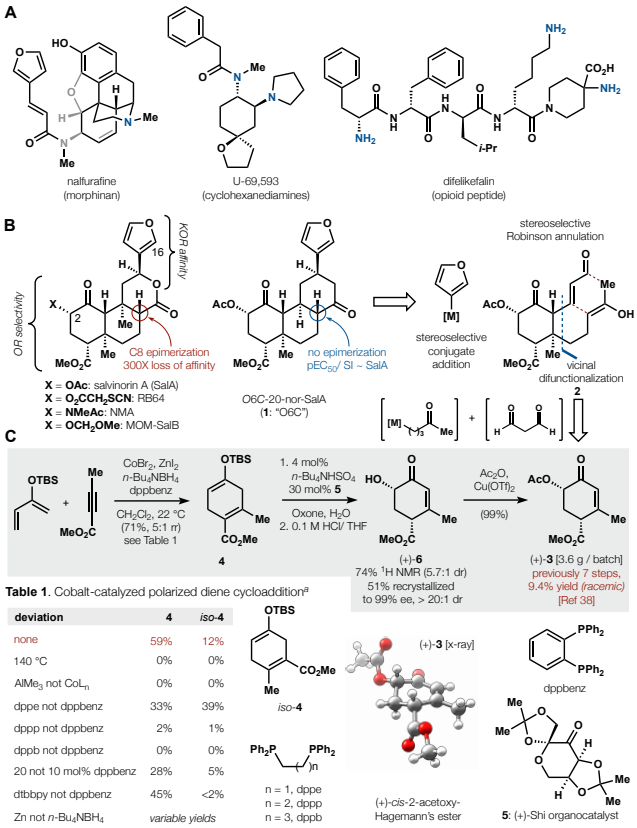

Table 1. Cobalt-catalyzed polarized diene cycloaddition[a]

deviation	4	*iso*-4
none	59%	12%
140 °C	0%	0%
$AlMe_3$ not CoL_n	0%	0%
dppe not dppbenz	33%	39%
dppp not dppbenz	2%	1%
dppb not dppbenz	0%	0%
20 not 10 mol% dppbenz	28%	5%
dtbbpy not dppbenz	45%	<2%
Zn not *n*-Bu_4NBH_4	*variable yields*	

Fig. 1. Salvinorin A, a KOR-selective hallucinogen, differs from common opioids. (**A**) KOR-selective opioid ligands that contain nitrogenous Brønsted bases. (**B**) Promising salvinorin A analogs, including the configurationally stable O6C and plan to effect Robinson annulation. (**C**) Synthesis entry that relies on control of regioselectivity in a cobalt-catalyzed cycloaddition. [a]optimized conditions: 10 mol% dppbenz, 10 mol% $CoBr_2$, 50 mol% ZnI_2, 0.3 equiv. *n*-Bu_4NBH_4, CH_2Cl_2 (0.5 M), 22 °C.

The synthesis commenced with a Diels-Alder reaction between two electronically matched partners. Neither high temperatures nor Lewis acids, however, promoted cycloaddition (entries 13 and 14 in Table 1) and attempts to access **4** via Birch reduction[26,27,28] proved unsuccessful. Only Hilt's cobalt-catalyzed cycloaddition[29] delivered 1,4-cyclohexadienes (65%), albeit as a ~1:1 ratio that favored regioisomer *iso*-**4**. Whereas many diphosphine ligands failed to promote reaction or regioselectivity, inexpensive dppBenz and 4,4'-di-*tert*-butylbipyridine (dtbbpy) ligands favored isomer **4**; the former provided higher yields. Zinc metal as reductant led to variable results on scale due to slow reduction rates in CH_2Cl_2, but tetrabutylammonium borohydride caused an immediate color change[30] and provided 71% yield with 5:1 rr over multiple large-scale runs (*ca.* 55 mmol; see Table S2 for optimization). The Co•dppBz complex enabled regioselective reaction of electronically matched, yet thermally unreactive, polarized diene-dienophile pairs; precedented conditions only used dienophiles with a pendant alkene ligand.[29,31] Selectivity may be dictated by either steric interactions in the regiochemistry-determining step by analogy to phenyl acetylene cycloadditions[32] or enhanced polarization of the butynoate•Co complex using the narrow bite-angle diphosphine (dppBz β_n = 83°) by analogy to metal hydricity trends.[33]

Enantioselective oxidation of **4** was explored using Jacobsen epoxidation and Sharpless dihydroxylation, but these conditions failed to engage the electron-rich alkene, as suggested by the absence of cyclohexenol silyl ethers in prior scope.[34,35] Fortunately, Shi epoxidation[36] (L-fructose-derived catalyst) effected Rubottom oxidation in 74% yield, 91:9 enantiomeric ratio and a 5.7:1 *cis*:*trans* diasteromeric ratio resulting from selective deconjugation of the ester. Recrystallization of this intermediate increased the er to over 99:1 and delivered **6** in 51% yield as a single diastereomer. This Hagemann's ester analog, **6**, proved sensitive to epimerization or aromatization under basic conditions, but could be converted quantitatively to the C2 acetate with catalytic $Cu(OTf)_2$ in neat acetic anhydride on multigram scale.[37] Prior analysis had suggested **3** as an entry to the enantioselective synthesis of the salvinorins.[38] Its synthesis, however, required 9 steps, relied on a stoichiometric ephedrine chiral auxiliary to reach scalemic intermediates, and eventually yielded *rac*-**3** only. In comparison, the entry in Figure 1 required four steps and a chiral catalyst to produce near-enantiopure (+)-**3**.

Previous work had established a procedure for the vicinal difunctionalization of Hagemann's ester,[24] yet these conditions and numerous iterations failed in the presence of the C2–O substituent, which rendered the ketone more sensitive to strong base and deactivated the already hindered, β-trisubstituted enolate likely via π_{CC}–σ^*_{CO} conjugation. After extensive optimization, we found that organocopper addition to the base-sensitive, hindered enone occurred most efficiently in the presence of trimethylsilyl trifluoromethanesulfonate (TMSOTf) as a powerful activator to accelerate oxidative addition of organocopper reagents.[39] Further screening identified diethyl ether as a cosolvent crucial for diastereoselectivity; in its absence, **10** added to the opposite face of the enone predominantly. Low-temperature quench with aqueous ammonium chloride prevented the side-reactions of excess **10** that occurred upon warming and spared the C6 enol silane, which showed stability even to chromatography on acidic silica gel, a result of its low nucleophilicity. Direct evidence of the low reactivity of the C6 position emerged during attempted *C*-allylation: treatment of enol silane **7** with diallyl carbonate, $Pd_2(dba)_3$•$CHCl_3$ and dppe at 60 °C yielded the *O*-allyl ether **8** instead of the *C*-allyl ketone **9** (11.4:1 **8**:**9**), whereas similarly hindered cyclohexenyl allyl carbonates have led to *C*-allyation exclusively.[40] This reaction sequence vividly illustrated the low reactivity of C6. Claisen rearrangement (*O*- to *C*-allyl, **8** to **9**) and multiple functional group interconversions (FGIs) could adapt the unfunctionalized allyl group to suit the synthesis (**9** to **2b**, **2b** to **2a**), but this sequence consumed time, labor and material.

Instead, we considered Reformatsky variants recently shown to couple ketone-aldehyde pairs that were unreactive under basic or Lewis acidic conditions.[41] Despite the low reactivity of **7**, *N*-iodosuccinimide effected high-yielding and diastereoselective α-halogenation on gram-scale (95%, >20:1 dr, 1 g per batch; see **11** X-ray); iodide **11** proved stable to thiosulfate workup,

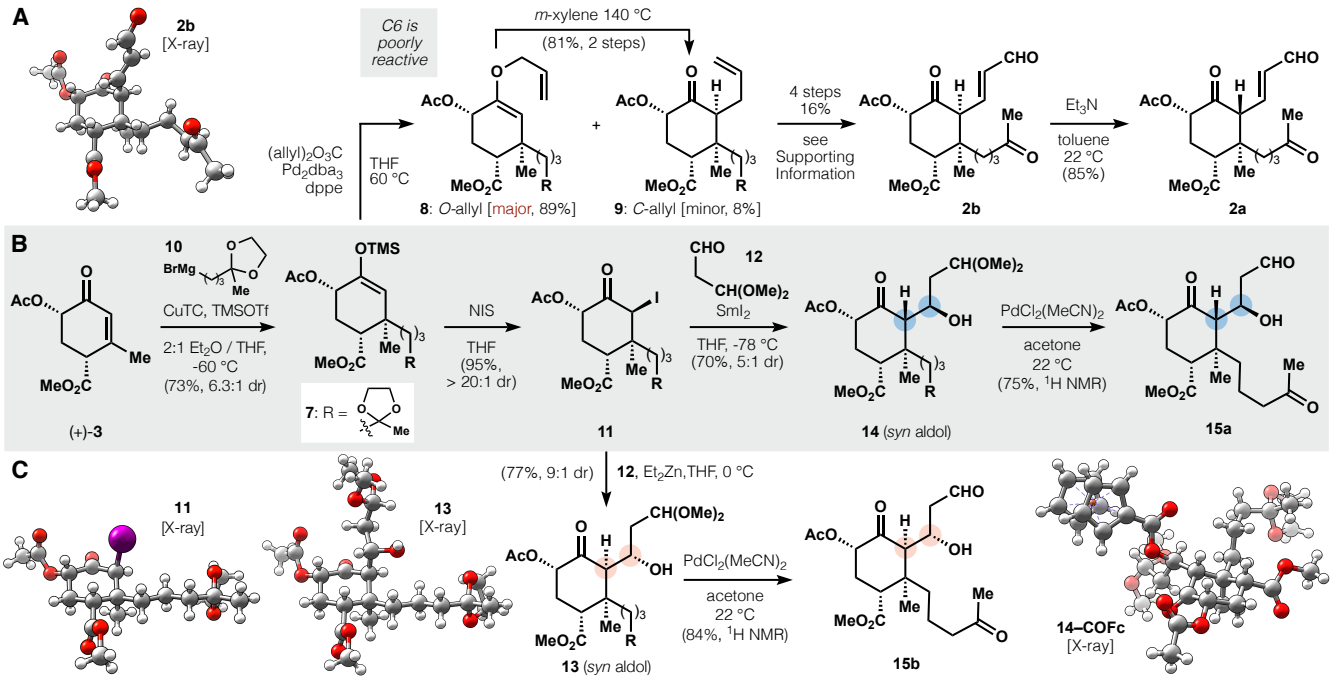

Fig. 2. Vicinal difunctionalization of 3. (**A**) The low reactivity of C6 prevents direct C–C bond formation. (**B**) Sm-Reformatsky aldol allows efficient sidechain appendage with equatorial syn-selectivity. (**C**) Zn-Refortmatsky reserves selectivity to an axial

chromatography and crystallization (Et_2O, -20 °C). Nevertheless, **11** underwent efficient Reformatsky reaction with malondialdehyde dimethylacetal (**12**) under the action of diethylzinc (Et_2Zn) to yield the *syn*-aldol diastereomer in an axial orientation (77%, 9:1 dr; see **13** X-ray). Whereas *E*-enolates tend to yield *syn*-aldols via open (Noyori) transition states, the absence of strong Lewis acid here suggests a closed (Zimmerman-Traxler) transition state where the aldehyde alkyl chain is forced into an axial approach (enolate *re*-face) by the enolate β-substituents (see Figure S5).[42] The high stereoselectivity, however, proved problematic because axial diastereomer **13** could not be advanced in the synthesis (see Fig. 3 below). Fortunately, SmI_2 could replace Et_2Zn and retain *syn*-selectivity, but reverse the aldehyde approach (enolate *si*-face) to yield diastereomer **14** (70%, 5:1 dr; see **14-CoFc** X-ray). The origin of this reversal may involve samarium chelation[43] between the enolate C1 oxygen and C2 acetate to enforce aldehyde approach adjacent to the axial β-methyl. Double hydrolysis of the acetals required unusual conditions due to the sensitivity of aldehydes **15a** and **15b** to silica gel, aqueous work-up and residual acid: $PdCl_2(MeCN)_2$ in acetone[44] delivered keto-aldehydes after filtration through activated carbon, followed by evaporation. Thus, enone (+)-**3** could be stereoselectively functionalized in 4 steps with sidechains in the correct oxidation state for a tandem cyclization of both B and C rings.

Attempts to effect Robinson annulation of **15a** or **2a** met initially with failure due to the competitive reaction of their multiple carbonyls in preference to the methyl ketone. Standard reagents—amines, acids and bases—first engaged α,β-unsaturated aldehydes **2a** and **2b** (Figure 3), produced from **15a** or **15b** by loss of water (identified in situ by comparison to the products of Figure 2A). Increased temperatures or reagent concentrations did not allow cyclization into structures like **16** and instead caused extensive decomposition, using either **15a** or **2a** generated independently. The low rate of cyclization and the tendency towards decomposition represented a dilemma: either the synthesis would require multiple steps to replace the linear methyl ketone with a superior nucleophile, or the linear methyl ketone would require selective enolization. Unfortunately, the enal sidechains could enolize with great ease, as demonstrated by the epimerization of **2b** to **2a** by Et_3N or SiO_2 at 22 °C (17:1, **2b**:**2a**). We turned to commercially-available chiral phosphoric acids, whose large substituents can dissociate reactivity from acidity[45,46] via non-covalent interactions[47] in flexible binding pockets.[48] Selective ketone binding and enolization, comparable to TRIP-AcOH host-guest binding,[47] might avoid reaction of bulkier Lewis basic motifs prone to decomposition, like the enolizable C6 ketone or ionizable C2 acetate. Phosphoric acids with no or minimal ortho-substitution—BPA ($pK_{a(DMSO)}$ = 3.37[49]) and o,o'-diphenyl-BPA ($pK_{a(DMSO)}$ = 3.86[49])—led to only trace product. However, 2,4,6-tricylohexylphenyl- (TCYP), 2,4,6-tri-iso-propylphenyl- (TRIP, $pK_{a(DMSO)}$ = 4.22[49]) and triphenylsilyl- ((R)- or (S)-TiPSY, $pK_{a(DMSO)}$ = est. 4.42[46]) substituents provided increasing amounts of Robinson annulation, ultimately delivering an 85% yield (18:1:2:2 dr) favoring **17a** over 3 other diastereomers (**17b–d**). All phosphoric acids solubilized completely under the reaction conditions and led to full consumption of starting materials. Small acids with lower, similar and higher $pK_{a(DMSO)}$ values (TsOH, 0.9;[50] Ph_2PO_4H, 3.88;[49] fumaric acid, 9.0[51]) led to decomposition. To distinguish between selective methyl ketone enolization versus capture of the enal-enol equilibrium (i.e. **2a** ⇋ **16** ⇋ **2b**), we subjected **15b** to identical conditions—(R)- or (S)-TiPSY or BPA, 30 mol%, PhCl, 85 °C. Isomer **2b** proved less sensitive to decomposition than **2a** (see BPA entries) but cyclized to **17d** only, despite the ability of **2b** to enolize with Et_3N and SiO_2. That the phosphoric acid enantiomeric series had only a small effect on both reaction efficiency and stereoselectivity suggested dissociation from the enol prior to cyclization.[52]

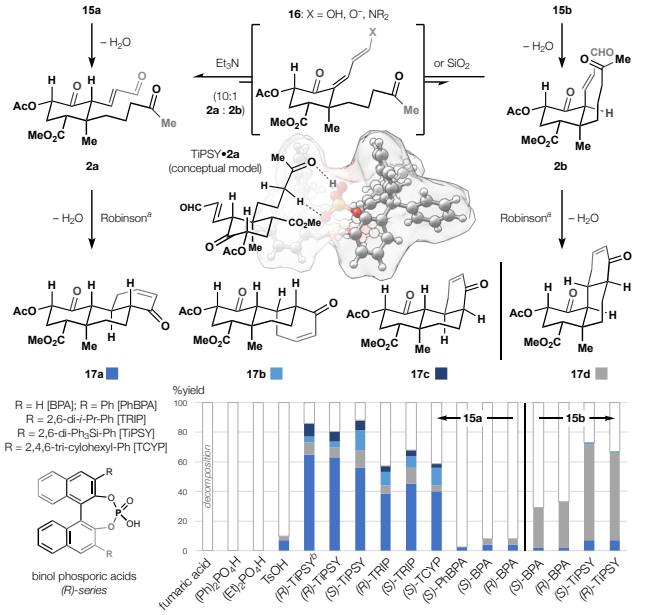

Fig. 3. Robinson annulation by selective enolization. Chiral binol-phosphoric acids with large o,o'-substituents enolize the weakly acidic, unhindered ketone but spare the highly acidic, hindered keto-enal. Empty bars indicate decomposition, not residual starting materials. [a]30 mol% acid catalyst, 0.1 M **15a** or **15b**, PhCl, 85°C; [b]toluene not PhCl.

Selective enolization of ketones is precedented in special cases where A(1,3)-strain reduces the competitive, kinetic acidity of low pKa 1,3-dicarbonyls;[53] that situation does not appear relevant here and the selectivity imparted by bulky phosphoric acids, as monomers or aggregates,[54] appears unprecedented.

To evaluate the practicality of the synthesis, we probed the ease with which we could assemble a focused library of bioactive congeners. Robinson annulation product **17a** could be advanced to O6C (**1**, Figure 4A) by diastereoselective Hayashi conjugate addition using $[Rh(COD)(OH)]_2$ with QuinoxP* to disfavor the C12 epimer, which predominated with other phosphines or organocopper nucleophiles via a proposed Fürst-Plattner model of stereoselectivity (see Figure S9). Selective access to the C12(*R*) configuration using QuinoxP* was restricted to electron-rich heterocyclic boronic acids, whereas electron-neutral phenyls required *(R)*-BINAP and electron-deficient relied on BenzP* in *t*-BuOH for high diastereoselectivity (see Table S7); these optimizations benefited from ready access to enone **17a**. The final conjugate addition completed a 10-step synthesis of O6C and accessed 29 other unprecedented analogs, including heteroaromatics and substituted phenyls. No conditions produced C8 epimers, by virtue of the designed scaffold stability of O6C (**1**) itself.[24,25]

Seminal work by Prisanzano established the importance of the C12 furan and its potential replacement with a series of aryl ketones via oxidation and Liebeskind-Srogl coupling.[55] Nevertheless, this C12 series led only to losses in potency, in contrast to widely explored C2 analogs.[12,56] The absence of experimental SalA•KOR structural data leaves many questions about important binding site contacts. We assayed[7] diverse carbocycle substitutions to determine whether hydrogen bonding, cation-π interactions or lipophilic contacts played important roles (Figure 4B). Prior binding models suggested a hydrogen bond in this region as necessary for high potency;[57] a recent furan-to-phenyl replacement retained affinity but lost potency.[24] To probe in-plane hydrogen bonding, we replaced the 3-furyl with strong acceptors[58] like 3- and 4-pyridyl (**20**-**21**), but these led to potency losses (Figure 4C). Instead, 3-thiophenyl (**19**) and phenyl (**25a**) led to increased potency, which might have suggested important cation-π or π-π interactions[59] perpendicular to the plane of the electron-rich rings. Investigation of this possibility was challenged by the sensitivity of potency to steric substitution (**23, 25**–**27**), so methyl-/chloro- isosteres (**28**–**31**) were used to make small, polar perturbations. Like the electron-rich furan/thiophene rings, the electron-deficient 3-chlorophenyl (**31**) exhibited high potency; this apparent contradiction suggested that lipophilic interactions—not H-bonds or π-interactions—likely played a dominant role. Indeed, replacement of the 3-furyl with a 1-hexenyl substituent (**32**) dramatically increased potency 20-fold (EC_{50} = 0.3 nM) and surpassed that of SalA itself. Thiophenol 1,4-addition led to a thioether (**33**, EC50 = 96 nM) that indicated a facile entry to diversity via commercially available thiols.

The C11 ketone showed greater tolerance for variation. Ring-expanded lactone and lactam analogs (**34**, **35**) retained good potency, as did oximes (**36**–**38**), easily accessible via condensation. Tertiary and secondary alcohols also proved potent and selective, especially **41b** (EC_{50} = 0.4 nM), which also exceeded SalA potency. The alkynylated analogs may prove useful for the recently reported CATCH protocol,[60] which requires active alkyne analogs for visualization of cellular and subcellular binding sites. Both alcohols and oximes offer prodrug functionalization sites to tune pharmacokinetics without alteration A-ring motifs (C2 acetate, ethers or *N*-methyl-acetamide) that govern affinity, selectivity and metabolism. SalA is highly selective for KOR over MOR and the analogs preserve, or in some cases improve upon, this selectivity profile, apparently a general feature of the O6C scaffold (see Figure S2 for MOR activity comparisons). Remarkably, multiple analogs display G protein signaling biased agonism; especially **34**, **37** and **40a**,**b** (bias factor 7.4–9.8, comparable to 16-Br-SalA), measured as potency of Gai protein-mediated inhibition of forskolin-stimulated cAMP accumulation versus βarrestin2 recruitment, both normalized to U69,593. Notably, compound **37** (cAMP pEC_{50} = 9.38 vs. βarr2 pEC_{50} = 7.37) relied on both the C12 phenyl and C11 oxime to expand its G protein bias; high selectivity for KOR over MOR was also preserved (Figure S2). The relative scarcity of G protein biased salvinorins in the literature suggests that this highly KOR-selective set represents a privileged area of chemical space to explore.

The salvinorins represent unique chemotypes for development of KOR-selective analgesics and antipruritics, most notably for their non-basic, high Fsp^3 scaffolds. The recreational use of *S. divinorum*, however, has led to restrictions in 32 US states and 20 countries, limiting access to plant-sourced materials for broad-development.[61] The synthesis reported here quickly enters the chemical space of salvinorin A and accesses new analogs at C11 and C12 that exceed the stability, potency, selectivity and G protein bias of the natural product itself. Whereas an early salvinorin analog, herkinorin, exhibited the first example of MOR-selective G protein bias,[62] corresponding KOR-selective biased agonists have proven harder to develop; the prevalence of functional bias in Figure 4C bodes well for

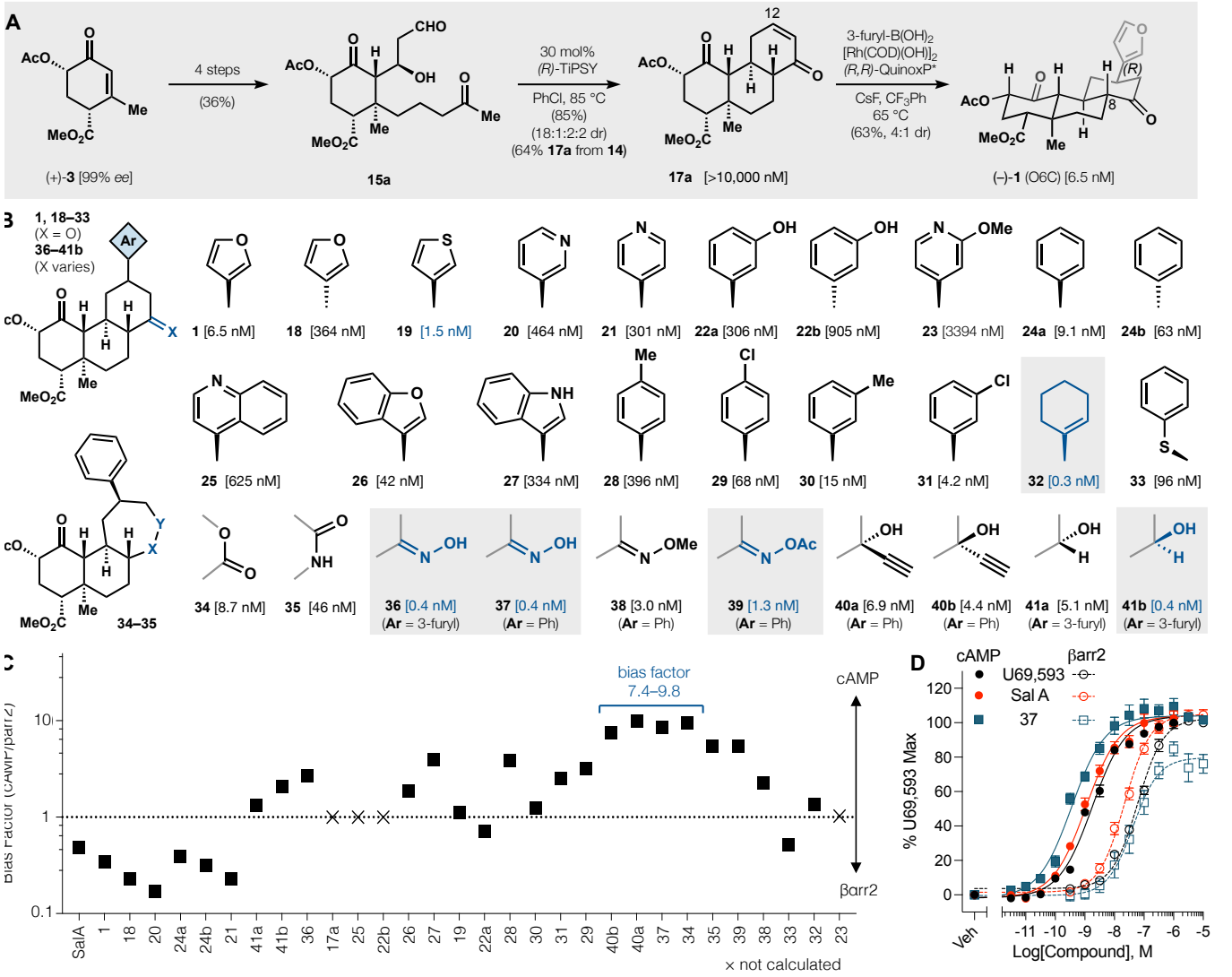

Fig. 4. Pharmacology measures synthesis design and practicality. The synthesis could be judged by its ability to generate multiple analogs that exceeded the potency, stability, selectivity and functional bias of SalA. A. Overview of the synthesis and ste stereoselective 1,4-addition of 3-furyl. **B**. Focused library to probe SAR where bracketed concentrations denote mean EC_{50} of inhibition of forskolin-stimulated cAMP accumulation via KOR; n≥3(Cisbio HTRF)). For tables of pharmacology data and plotted curves, see Figures S1-S2 and Table S1. **C**. Bias factors $[10^{\wedge(\Delta\Delta\log(\tau/KA)(cAMP-\beta arr2))}]$ for SalA and analogs. **D**. Representative CRCs of select analog **37** vs. positive controls U69,593 and SalA in cAMP and βarrestin2 (DiscoveRx PathHunter) signaling assays; data are normalized to the baseline and the maximum response produced by 10 μM U69,593 and are presented as the mean ± SEM.

further discovery. Key to this discovery platform were 1) cobalt-catalyzed access to a scalemic Hagemann's ester derivative; 2) stereoselective Reformatsky to overcome low enolate reactivity and 3) enolization of an unactivated ketone in the presence of an unstable electrophile to effect a stereoselective Robinson annulation cascade. Diverse salvinorins can now be accessed by concise total synthesis, placing a rational medicinal chemistry campaign within reach.

ASSOCIATED CONTENT

Supporting Information

All data is made available in the main text or the Supporting Information, including experimental procedures, copies of NMR spectra, X-ray structure reports, full outlines of prior syntheses and all pharmacological protocols. Structural parameters for X-ray crystal structures are available from the Cambridge Crystallographic Data Centre (**3**: CCDC2202073; **6**: CCDC2195935; **11**: CCDC2211512; **S5**: CCDC2241886; **13**: CCDC2245372; **17b**: CCDC2250953; **17c**: CCDC2217612; **1**: CCDC2249326; **S6**: CCDC2127086; **2b**: CCDC2166577)

ACKNOWLEDGMENT

We thank Jingyang Shi (Lanzhou University) and Wilson Lubeck (University of California, San Diego) for early contributions. Arnold Rheingold, Milan Gembicky, Jake Bailey and Erika Samolova are thanked for X-ray crystallographic analysis. We gratefully acknowledge Jason S. Chen and the Scripps Automated Synthesis facility (ASF) for help with analysis and separations, and Dee-Hua Huang and Laura Pasternack for NMR assistance. We thank Sophie Shevick, Tucker Huffman and Cheng Bi for helpful discussions. We thank the NIDA Drug Supply Program for providing buprenorphine used as a control for MOR in the Supporting Information.

REFERENCES

1. A. G. Atanasov *et al.* Natural products in drug discovery: advances and opportunities. *Nat. Rev. Drug Discov.* **20**, 200–216 (2021).
2. B. L. Roth BL, K. Baner, R. Westkaemper, D. Siebert, K. C. Rice, S. Steinberg, P Ernsberger, R. B. Rothman, Salvinorin A: a potent naturally occurring nonnitrogenous κ opioid selective agonist. *Proc. Natl. Acad. Sci. USA* **99**, 11934–11939 (2002).
3. A. Hopkins, G. Keserü, P. Leeson, D. C. Rees, C. H. Reynolds, The role of ligand efficiency metrics in drug discovery. *Nat Rev Drug Discov.* **13**, 105–121 (2014).
4. J. M. Hooker, Y. Xu, W. Schiffer, C. Shea, P. Carter, J. S. Fowler, Pharmacokinetics of the potent hallucinogen, salvinorin A in primates parallels the rapid onset and short duration of effects in humans. *Neuroimage* **41**, 1044–1050 (2008).
5. J. J. Roach, R. A. Shenvi, A review of salvinorin analogs and their kappa-opioid receptor activity. *Bioorg. Med. Chem. Lett.* **28**, 1436–1445 (2018).
6. L. M. Bohn, J. Aubé, Seeking (and finding) biased ligands of the kappa opioid receptor. *ACS Med. Chem. Lett.* **8**, 694–700 (2017).
7. J.-H. Ho, E. L. Stahl, C. L. Schmid, J. Aubé, L. M. Bohn, G protein signaling–biased agonism at the κ-opioid receptor is maintained in striatal neurons. *Sci. Signal.* **11**, eaar4309 (2018).
8. Z. S. Teksin, I. J. Lee, N. N. Nemieboka, A. A. Othman, V. V. Upreti, H. E. Hassan, S. S. Syed, T. E. Prisinzano, N. D. Eddington, Evaluation of the transport, in vitro metabolism and pharmacokinetics of Salvinorin A, a potent hallucinogen. *Eur. J. Pharm. Biopharm.* **72**, 471–477 (2009).
9. J. M. Hooker, T. A. Munro, C. Béguin, D. Alexoff, C. Shea, Y. Xu, B. M. Cohen, Salvinorin A and derivatives: protection from metabolism does not prolong short-term, whole-brain residence. *Neuropharmacology* **57**, 386–391 (2009).
10. C. Beguin, D. N. Potter, J. A. DiNieri, T. A. Munro, M. R. Richards, T. A. Paine, L. Berry, Z. Zhao, B. L. Roth, W. Xu, L. Y. Liu-Chen, N-methylacetamide analog of salvinorin A: A highly potent and selective κ-opioid receptor agonist with oral efficacy. *J. Pharm. Exper. Ther.* **324**, 188–195 (2008).
11. T. E. Prisinzano, R. B. Rothman, Salvinorin A analogs as probes in opioid pharmacology. *Chem. Rev*. **108**, 1732–1743 (2008).
12. K. L. White, J. E. Robinson, H. Zhu, J. F. DiBerto, P. R. Polepally, J. K. Zjawiony, D. E. Nichols, C. J. Malanga, B. L. Roth, The G protein–biased κ-opioid receptor agonist RB-64 is analgesic with a unique spectrum of activities in vivo. *J. Pharmacol. Exp. Ther.* **352**, 98–109, (2015).
13. K. F. Paton, A. Biggerstaff, S. Kaska, R. S. Crowley, A. C. La Flamme, T. E. Prisinzano, B. M. Kivell, Evaluation of biased and balanced salvinorin A analogs in preclinical models of pain. *Front Neurosci.* **14**, 1–13 (2020).
14. J. R. Scheerer, J. F. Lawrence, G. C. Wang, D. A. Evans, Asymmetric synthesis of salvinorin A, a potent κ opioid receptor agonist. *J. Am. Chem. Soc.* **129**, 8968–8969 (2007).
15. M. Nozawa, Y. Suka, T. Hoshi, T. Suzuki, H. Hagiwara, Total synthesis of the hallucinogenic neoclerodane diterpenoid salvinorin A. *Org. Lett.* **10**, 1365–1368 (2008).
16. H. Hagiwara, Y. Suka, T. Nojima, T. Hoshi, T. Suzuki, Second-generation synthesis of salvinorin A. *Tetrahedron* **65**, 4820–4825 (2009).
17. N. J. Line, A. C. Burns, S. C. Butler, J. Casbohm, C. J. Forsyth, Total Synthesis of (−)-Salvinorin A. *Chem. Eur. J.* **22**, 17983–17986 (2016).
18. Y. Wang, P. Metz, Total Synthesis of the Neoclerodane Diterpene Salvinorin A via an Intramolecular Diels–Alder Strategy. *Org. Lett.* **20**, 3418–3421 (2018).
19. Halang, M.; Maier, M. E. Formal Total Synthesis of Salvinorin A. *ChemistryOpen* **11**, e202200015 (2022).
20. Zimdars, P.; Wang, Y.; Metz, P. A Protecting-Group-Free Synthesis of (−)-Salvinorin A. *Chem. Eur. J.* **27**, 7968–7973 (2021).
21. Y. E. Bergman, R. Mulder, P. Perlmutter, Total synthesis of 20-norsalvinorin A. 1. Preparation of a key intermediate. *J. Org. Chem.* **74**, 2589–2591 (2009).
22. S. J. Hill, A. U. C. M. Brion, R. A. Shenvi, Chemical syntheses of the salvinorin chemotype of KOR agonist. *Nat. Prod. Rep*. **37**, 1478–1496 (2020).
23. A. M. Sherwood, S. E. Williamson, R. S. Crowley, L. M. Abbott, V. W. Day, T. E. Prisinzano, Modular Approach to pseudo-Neoclerodanes as Designer κ-Opioid Ligands. *Org. Lett.* **19**, 5414–5417 (2017).
24. J. J. Roach, Y. Sasano, C. L. Schmid, S. Zaidi, V. Katrich, R. C. Stevens, L. M. Bohn, R. A. Shenvi, Dynamic strategic bond analysis yields a ten-step synthesis of 20-nor-Salvinorin A, a potent κ-OR agonist. *ACS Cent. Sci.* **3**, 1329–1336 (2017).
25. S. Hirasawa, M. Cho, T. F. Brust, J. J. Roach, L. M. Bohn, R. A. Shenvi, O6C-20-nor-salvinorin A is a stable and potent KOR agonist. *Bioorg. Med. Chem. Lett.* **28**, 2770–2722 (2018).
26. J. Burrows, S. Kamo, K. Koide, Scalable Birch reduction with lithium and ethylenediamine in tetrahydrofuran. *Science* **374**, 741-746 (2021).
27. B. K. Peters, K. X. Rodriguez, S. H. Reisberg, S. B. Bell *et al.* Scalable and safe synthetic organic electroreduction inspired by Li-ion battery chemistry. *Science* **363**, 838–845 (2019).
28. P. Lei, Y. Ding, X. Zhang, A. Adijiang, H. Li, Y. Ling, J. An, J. A practical and chemoselective ammonia-free Birch reduction. *Org. Lett.* **20**, 3439–3442 (2018).
29. G. Hilt, J. Janikowski, W. Hess, *meta*-Directing Cobalt-Catalyzed Diels–Alder Reactions. *Angew. Chem. Int. Ed.* **45**, 5204 –5206 (2006).

30. G. Hilt, F.-X. du Mesnil, An improved cobalt catalyst for homo Diels–Alder reactions of acyclic 1,3-dienes with alkynes. *Tetrahedron Lett.* **41**, 6757–6761 (2000).
31. F. Erver, J. R. Kuttner, G. Hilt, Multidirectional Cobalt-Catalyzed Diels–Alder/1,4-Hydrovinylation Sequences. *J. Org. Chem.* **77**, 8375–8385 (2012).
32. P. Mörschel, J. Janikowski, G. Hilt, G. Frenking, G. Ligand-Tuned Regioselectivity of a Cobalt-Catalyzed Diels−Alder Reaction. A Theoretical Study. *J. Am. Chem. Soc.* **130**, 8952–8966 (2008).
33. J. W. Raebiger, A. Miedaner, C. J. Curtis, S. M. Miller, O. P. Anderson, D. L. DuBois, Using ligand bite angles to control the hydricity of palladium diphosphine complexes. *J. Am. Chem. Soc.* **126**, 5502–5514 (2004).
34. E. N. Jacobsen, W. Zhang, A. R. Muci, J. R. Ecker, L. Ding, L. Highly enantioselective epoxidation catalysts derived from 1, 2-diaminocyclohexane. *J. Am. Chem. Soc.* **113**, 7063–7064 (1991).
35. W. Adam, R. T. Fell, V. R. Stegmann, C. R. Saha-Möller, Synthesis of Optically Active α-Hydroxy Carbonyl Compounds by the Catalytic, Enantioselective Oxidation of Silyl Enol Ethers and Ketene Acetals with (Salen)manganese(III) Complexes. *J. Org. Chem.* **120**, 708–714 (1998).
36. Z.-X. Wang, Y. Tu, M. Frohn, J. R. Zhang, Y. Shi, An efficient catalytic asymmetric epoxidation method. *J. Am. Chem. Soc.* **119**, 11224–11235 (1997).
37. P. Saravanan, V. K. Singh, An efficient method for acylation reactions. *Tetrahedron Lett.* **40**, 2611–2614 (1999).
38. A. R. Lingham, H. M. Hügel, T. J. Rook, Studies towards the synthesis of salvinorin A. *Aust. J. Chem.* **59**, 340–348 (2006).
39. M. Rodríguez-Fernández, X. Yan, J. F. Collados, P. B. White, S. R. Harutyunyan, Lewis acid enabled copper-catalyzed asymmetric synthesis of chiral β-substituted amides. *J. Am. Chem. Soc.* **139**, 14224–14231 (2017).
40. F. Horeischi, N. Biber, B. Plietker, B. The Total Syntheses of Guttiferone A and 6-*epi*-Guttiferone A. *J. Am. Chem. Soc.* **136**, 4026–4030 (2014).
41. M. A. Baker, R. M. Demoret, M. Ohtawa, R. A. Shenvi, R. A. Concise asymmetric synthesis of (−)-bilobalide. *Nature*, **575**, 643–646 (2019).
42. J. Matsuo, M. Murakami, The Mukaiyama aldol reaction: 40 years of continuous development. *Angew. Chem. Int. Ed.* **52**, 9109–9118 (2013).
43. M. Sinast, M. Zuccolo, J. Wischnat, T. Sube, F. Hasnik, A. Baro, S. Dallavalle, S. Laschat, Samarium iodide-promoted asymmetric reformatsky reaction of 3-(2-haloacyl)-2-oxazolidinones with enals. *J. Org. Chem.* **84**, 10050–10064 (2019).
44. B. H. Lipshutz, D. Pollart, J. Monforte, H. Kotsuki, Pd (II)-catalyzed acetal/ketal hydrolysis/exchange reactions. *Tetrahedron Lett.* **26***,* 705–708 (1985).
45. K. Rothermal, M. Melikian, J. Hioe, J. Greindl, J. Gramüller, M. Žabka, N. Sorgenfrei, T. Hausler, F. Morana, R. M. Gschwind, Internal acidity scale and reactivity evaluation of chiral phosphoric acids with different 3, 3′-substituents in Brønsted acid catalysis. *Chem. Sci.* **10**, 10025–10034 (2019).
46. C. Yang, X.-S. Xue, J.-L. Jin, X. Li, J. P. Cheng, Theoretical study on the acidities of chiral phosphoric acids in dimethyl sulfoxide: hints for organocatalysis. *J. Org. Chem.* **78**, 7076–7085 (2013).
47. M. R. Monaco, B. Poladura, M. Diaz de Los Bernardos, M. Leutzsch, R. Goddard, B. List, Activation of carboxylic acids in asymmetric organocatalysis. *Angew. Chem. Int. Ed.,* **53**, 7063-7067 (2014).
48. L. Kötzner, M. J. Webber, A. Martínez, C. De Fusco, B. List, B. Asymmetric catalysis on the nanoscale: the organocatalytic approach to helicenes. *Angew. Chem. Int. Ed*. **53**, 5202–5205 (2014).
49. P. Christ, A. G. Lindsay, S. S. Vormittag, J. M. Neudörfl, A. Berkessel, A. C. O'Donoghue, pKa Values of Chiral Brønsted Acid Catalysts: Phosphoric Acids/Amides, Sulfonyl/Sulfuryl Imides, and Perfluorinated TADDOLs (TEFDDOLs). *Chem. Eur. J.* **17**, 8524–8528 (2011).
50. A. Borovika, P.-I. Tang, S. Klapman, P. Nagorny, Thiophosphoramide-based cooperative catalysts for Brønsted acid promoted ionic Diels–Alder reactions. *Angew. Chem. Int. Ed.* **52**, 13424–13428 (2013).
51. P. J. Choi, K. A. Petterson, J. D. Roberts, Ionization equilibria of dicarboxylic acids in dimethyl sulfoxide as studied by NMR. *J. Phys. Org. Chem*. **15**, 278-286 (2002).
52. R. J. Phipps, G. L. Hamilton, F. D. Toste, The progression of chiral anions from concepts to applications in asymmetric catalysis. *Nature Chem.* **4**, 603–614 (2012).
53. D. A. Evans, J. S. Clark, R. Metternich, V. J. Novack, G. S. Sheppard, Diastereoselective aldol reactions using. beta.-keto imide derived enolates. A versatile approach to the assemblage of polypropionate systems. *J. Am. Chem. Soc.* **112**, 866 (1990).
54. N. Li, X.-H. Chen, S.-M. Zhou, S.-W. Luo, J. Song, L. Ren, L.-Z. Gong, Asymmetric amplification in phosphoric acid catalyzed reactions. *Angew. Chem., Int. Ed.* **49**, 6378–6381 (2010).
55. K. M. Lovell, T. Vasiljevik, J. J. Araya, A. Lozama, K. M. Prevatt-Smith, V. W. Day, C. M. Dersch, R. B. Rothman, E. R. Butelman, M. J. Kreek, T. E. Prisinzano, Semisynthetic neoclerodanes as kappa opioid receptor probes. *Bioorg. Med. Chem.* **20**, 3100–3110 (2012).
56. T. A. Munro, K. K. Duncan, W. Xu, Y. Wang, L.-Y. Liu-Chen, W. A. Carlezon Jr, B. M. Cohen, C. Béguin, Standard protecting groups create potent and selective κ opioids: Salvinorin B alkoxymethyl ethers. *Bioorg. Med. Chem.* **16**, 1279–1286 (2008).
57. F. Yan, P. D. Mosier, R. B. Westkaemper, J. Stewart, J. K. Zjawiony, T. A. Vortherms, D. J. Sheffler, B. L. Roth, Identification of the molecular mechanisms by which the diterpenoid salvinorin A binds to κ-opioid receptors. *Biochemistry* **44**, 8643–8651 (2005).
58. I. Nobeli, S. L. Price, J. P. M. Lommerse, R. Taylor, Hydrogen bonding properties of oxygen and nitrogen

acceptors in aromatic heterocycles. *J. Comp. Chem.* **18**, 2060-2074 (1997).
59. K. Kumar, S. M. Woo, T. Siu, W. A. Cortopassi, F. Duarte, R. S. Paton, Cation–π interactions in protein–ligand binding: Theory and data-mining reveal different roles for lysine and arginine. *Chem. Sci.*, **9**, 2655–2665 (2018).
60. Z. Pang, M. A. Schafroth, D. Ogasawara, Y. Wang, V. Nudell, N. K. Lal, D. Yang, K. Wang *et al.* In situ identification of cellular drug targets in mammalian tissue. *Cell* **185**, 1793–1805.e17 (2022).
61. P.-X. Lin, J.-H. Li, S.-H. Chen, H.-C. Cheng, R. McKetin, Quantitative determination of salvinorin A, a natural hallucinogen with abuse liability, in Internet-available Salvia divinorum and endemic species of Salvia in Taiwan. *J. Food Drug Anal.* **22**, 370–378 (2014).
62. C. E. Groer, K. Tidgewell, R. A. Moyer, W. W. Harding, R. B. Rothman, T. E. Prisinzano, L. M. Bohn, An opioid agonist that does not induce μ-opioid receptor—arrestin interactions or receptor internalization. *Mol. Pharm.* **71**, 549–557 (2007).
63. C. L. Schmid, N. M. Kennedy, N. C. Ross, K. M. Lovell, Z. Yue, J. Morgenweck, M. D. Cameron, T. D. Bannister, L. M. Bohn, Bias Factor and Therapeutic Window Correlate to Predict Safer Opioid Analgesics. *Cell* **2017**, *171*, 1165-1175 e1113, doi:10.1016/j.cell.2017.10.035.
64. M. M. Vega, D. M. Crain, L. C. Konkol, R. J. Thomson, Enantioselective Synthesis of Metacycloprodigiosin via the 'Wasserman Pyrrole.' *Tetrahedron Lett.* **56** 3228–3230 (2015).
65. R. M. Moriarty, R. K. Vaid, V. T. Ravikumar, T. E. Hopins, P. Farid, Hypervalent iodine oxidation of 5-substituted and 4,5-disubstituted pyrazol-3(2H)-ones: A facile synthesis of methyl-2-alkynoates and methyl 2,3-alkadienoates. *Tetrahedron* **45** 1605-1610 (1989).
66. A. Narayanappa, D. Hurem, J. McNulty, Regioselective Ylide Formation on Acetal-Functionalized Trialkyl Phosphonium Salts: Extending the Scope of Carbonyl Homologation. *Synlett* **28**, 2961-2965 (2017).
67. L. Bi, Y. Zhang, M. Zhao, C. Wang, P. Chan, J. Tok, S. Peng, Novel synthesis and anti-inflammatory activities of 2,5-disubstituted-dioxacycloalkanes. *Bioorg. Med. Chem.* **13**, 5640-5646 (2005).
68. M-X. Zhao, Y. Shi, Practical synthesis of an L-fructose-derived ketone catalyst for asymmetric epoxidation of olefins. *J. Org. Chem.* **71**, 5377-5379 (2006).
69. T. F. Jamison, Y. Ikeuchi, Process for preparation of 1,2:4,5-bis-O-(1-methylethylidene)-β-L-erythro-2,3-hexodiulo-2,6-pyranose Patent WO 2011/109276 Al, September 9, 2011
70. K. Speck, R. Wildermuth, T. Magauer, Convergent Assembly of the Tetracyclic Meroterpenoid (−)-Cyclosmenospongine by a Non-Biomimetic Polyene Cyclization. *Angew. Chem.* **128**, 14337-14341 (2006).
71. W. G. Whitehurst, J. Kim, S. G. Koenig, P. J. Chirik, Three-Component Coupling of Arenes, Ethylene, and Alkynes Catalyzed by a Cationic Bis(phosphine) Cobalt Complex: Intercepting Metallacyclopentenes for C–H Functionalization. *J. Am. Chem. Soc.* **144**, 4530–4540 (2022).
72. A. J. Birch, *J. Chem. Soc.* 430-436 (1944).
73. P. Lei, Y. Ding, X. Zhang, A. Adijiang, H. Li, Y. Ling, An, J. A Practical and Chemoselective Ammonia-Free Birch Reduction. *Org. Lett.* **20**, 3439–3442 (2018).
74. B. K. Peters, et al. Scalable and safe synthetic organic electroreduction inspired by Li-ion battery chemistry. *Science* **363**, 838-845 (2019).
75. J. Burrows, S. Kamo, K. Koide, Scalable Birch reduction with lithium and ethylenediamine in tetrahydrofuran. *Science*, **374**, 741-746 (2021).
76. B. F. Marcune, S. Karady, U. H. Dolling, T. J. Novak, Methoxymethylation of Alcohols, Phenols, and Avermectin Aglycones Using MOM-2-pyridylsulfide. *J. Org. Chem.* **64**, 2446–2449 (1999).
77. L. Wang, Y. Hashidoko, M. Hashimoto, Cosolvent-Promoted O-Benzylation with Silver(I) Oxide: Synthesis of 1′-Benzylated Sucrose Derivatives, Mechanistic Studies, and Scope Investigation. *J. Org. Chem.* **81**, 4464–4474 (2016).
78. K. W. C. Poon, S.E. House, G. B. Dudley, A Bench-Stable Organic Salt for the Benzylation of Alcohols. *Synlett* **20**, 3142-3144 (2005).
79. O. Yasunori, O. Mamiko, B. Masafumi, Y. Hidetoshi, Benzyl N-Phenyl-2,2,2-trifluoroacetimidate: A New and Stable Reagent for O-Benzylation. *Chem. Lett.* **36**, 992-993 (2007).
80. N. Asao, H. Aikawa, S. Tago, K. Umetsu, Gold-Catalyzed Etherification and Friedel−Crafts Alkylation Using ortho-Alkynylbenzoic Acid Alkyl Ester as an Efficient Alkylating Agent. *Org. Lett.* **9**, 4299–4302 (2007).
81. G. Bartoli, M. Bosco, M. Locatelli, E. Marcantoni, P. Melchiorre, L. Sambri, Unusual and Unexpected Reactivity of t-Butyl Dicarbonate (Boc2O) with Alcohols in the Presence of Magnesium Perchlorate. A New and General Route to t-Butyl Ethers. *Org. Lett.* **7**, 427–430 (2005).
82. J. Otera, N. Danoh, H. Nozaki, Novel template effects of distannoxane catalysts in highly efficient transesterification and esterification. *J. Org. Chem.* **56,** 5307–5311 (1991).
83. B. Ye, J. Yao, C. Wu, H. Zhu, W. Yao, L. Jin, X. Dou, Rhodium-Catalyzed Asymmetric Conjugate Pyridylation with Pyridylboronic Acids. *ACS Catal.* **12** 2434–2440 (2022).
84. A. Lingham, Studies Toward the Synthesis of Salvinorin A. Royal Melbourne Institute of Technology, Melbourne, Australia (2007).